AFM Study of the Breakup of Catalyst Particles during Ethylene Polymerization

V. J. Ruddick and J. P. S. Badyal*

Department of Chemistry, Science Laboratories, Durham University, Durham DH1 3LE, England, U.K.

Received: October 17, 1996; In Final Form: December 25, 1996[⊗]

Atomic force microscopy has been used to follow the breakup of catalyst particles and the growth of polymer during ethylene polymerization over the Phillips CrO_x/silica calalyst.

Introduction

Heterogeneous polymerization catalysts require well-designed support materials that are capable of undergoing fragmentation during reaction while possessing the strength to withstand high-temperature activation procedures (e.g., calcination).[1,2] Fragmentation is necessary in order to maintain monomer access to active catalytic sites located within the pores of the support.[3] Early studies of the Phillips CrO_x/silica catalyst system used high-temperature ashing of the product phase to leave behind fragmented support material, which was then examined by BET and mercury porosimetry methods.[4] Artifacts introduced during the ashing procedure were later shown to render the results from these studies as unreliable.[5] More recently, SEM/TEM,[2,3,6,7] X-ray microscopy,[8,9] and synchrotron microtomography techniques have been employed to observe the fragmentation processes occurring during polymerization, and the changing porosity of the catalyst material has been investigated using mercury porosimetry[10] and pulse solid−gas chromatography.[11] These techniques suffer from many drawbacks (for example, SEM and TEM require the application of a conductive coating to the particle) that may influence the topography of the particles; synchrotron microtomography requires access to a synchrotron source, mercury porosimetry may itself cause the support to breakup, and pulse solid−gas chromatography is strongly dependent upon elution dynamics.

Atomic force microscopy (AFM) is widely used to image the surfaces of solid materials.[12] It works by scanning a very sharp tip across a sample surface and measuring the forces of interaction between the tip and the substrate. Tapping mode and phase-imaging[13,14] AFM are useful variations of this technique. The former employs an etched silicon cantilever that is made to oscillate at a frequency close to its resonance frequency by a piezoelectric driver; the surface topography is imaged by measuring the drop in oscillation amplitude as the tip lightly "taps" the surface. Phase-imaging AFM compares the phase of the cantilever oscillation with that of the piezoelectric driver; the measured phase lag is dependent upon the composition of the sample: a softer sample exhibits a larger phase lag relative to a hard one.[13] Tapping mode and phase-imaging AFM can be run simultaneously, thereby offering topographical and compositional data for the same scan area. To be able to image small particles by AFM, certain limitations must be overcome. First, the particles need to be fixed firmly onto a substrate. Another problem arises if the feature being imaged is of comparable dimensions to the tip. If this is the case, then as the probe tip scans across the particles, the edge of the tip is imaged rather than the feature.[15] Both these drawbacks can be overcome by partially embedding the particle in a thermoplastic adhesive.[16] The particle then appears flatter during imaging, since most of its bulk lies beneath the surface of the adhesive and it is kept still.

In the present study, the breakup of the Phillips CrO_x/silica catalyst during ethylene polymerization has been followed by contact mode, tapping mode, and phase-imaging AFM. Previous mercury porosimetry[10] and pulse solid−gas chromatography[8] studies have indicated that polymer fills the support macropores first, while SEM/TEM[2,3,6,7] and X-ray microscopy[8,9] have shown that the support fragments in a nonuniform manner, the larger particles being observed at the external surfaces of the polymer particles. AFM overcomes the prerequisite for a conducting coating, and it should provide topographical information on dimension scales that are inaccessible to previously reported techniques.

Experimental Section

Basic chromium(III) acetate was aqueously impregnated onto silica support material (Crosfield Limited, surface area = 323 $m^2\ g^{-1}$, pore volume = 1.81 $cm^3\ g^{-1}$, prepared by the sol−gel route) and dried. A quantity of 1 g of material was placed into a quartz microreactor tube. Oxygen carrier gas (BOC, 99.9% purity) was dried through a concentrated H_2SO_4 bubbler followed by a P_2O_5 drying column and then an activated 3A molecular sieve (Aldrich) column at a flow rate of 1.5 $dm^3\ h^{-1}$. The reactor tube was heated at 1 K min^{-1} up to 1053 K using a Eurotherm temperature controller and then held at this high temperature for 5 h prior to cooling at 5 K min^{-1} back to room temperature. The oxidized CrO_x/SiO_2 catalyst was then prereduced using carbon monoxide at 623 K for 15 min followed by exposure to high-purity ethylene (99.8%, Scott Speciality Gases) for 15 min at 383 K. This was found to be sufficiently short to ensure that a variety of catalyst particles at different stages of polymerization could be identified by AFM. The formation of white polyethylene granules was taken as being indicative of an active catalyst and was confirmed by Fourier transform infrared spectroscopy.[17]

Sample preparation for AFM characterization comprised of partially embedding particulate material into a thermoplastic adhesive.[16] Small pieces of cleaved mica (∼1 cm^2) were placed onto a hot plate at 393 K. Thermoplastic adhesive (Tempfix, Agar Scientific) was spread onto the mica substrates and cooled slowly to room temperature in order to create a smooth film. The powdered catalyst sample was then dusted onto the prepared adhesive substrate and placed in a vacuum oven at 363 K for 3.5 h. These conditions were found to partially embed the particles, thereby allowing imaging of the catalyst surface by AFM.

A Digital Instruments Nanoscope III atomic force microscope was used for contact mode, tapping mode, and phase-imaging AFM analysis of the partially embedded particles. AFM images were acquired in air at room temperature using a 100 μm × 100 μm piezoelectric scan head and are presented as unfiltered data. Contact mode images were collected using a 200 μm wide-legged silicon nitride cantilever with a low spring constant (k = 0.12 Nm^{-1}) to minimize surface damage due to high

* To whom correspondence should be addressed.

[⊗] Abstract published in *Advance ACS Abstracts,* February 1, 1997.

S1089-5647(96)03206-3 CCC: $14.00

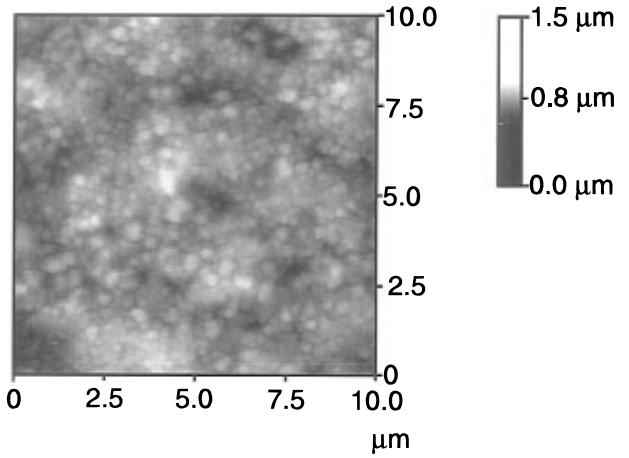

Figure 1. Contact mode AFM micrograph of the as-received silica support surface (the shaded bar is a measure of height).

contact forces. Tapping mode and phase-imaging AFM studies used a stiff silicon cantilever oscillating at close to its resonance frequency. Larger view images were taken at 10 and 100 μm to check that the smaller scale images were typical structures.

Results

Contact mode AFM analysis of the silica support showed that the surface of each particle consisted of an aggregation of spheroids ($\sim$0.31 $\pm$ 0.07 μm diameter) with pore openings evident across the surface (Figure 1). Phase-imaging AFM was used to check for the absence of any adhesive on the surface. The calcined CrO_x/silica catalyst is very similar in appearance to the silica support surface (spheroids of $\sim$0.26 $\pm$ 0.07 μm diameter). This can be taken as being an indication that sintering does not occur during calcination at 1053 K. Phase-imaging AFM showed only one phase to be present at the catalyst particle surface (as indicated by the absence of any significant color contrast in the phase image; see Figure 2a).

Exposure of the activated CrO_x/silica catalyst to ethylene resulted in the formation of white powder, which was identified by FTIR spectroscopy as being polyethylene.[17] Optical microscopy provided evidence for some agglomeration of polymerizing particles.[8,9,11] Contact mode AFM analysis during the very early stages of polymerization showed a surface that was very similar in appearance to that of the silica support material except that the spheroids were smaller ($\sim$0.14 $\pm$ 0.04 μm diameter) than those observed for either the silica support or the calcined catalyst. It can be seen by phase-imaging AFM that the ragged appearance of the catalyst phase image gradually breaks up with increasing levels of polymerization (the polymer exhibits a much smoother phase image; see Figure 3). This is accompanied by polymer starting to appear in cracks extending from pores (Figure 3). Eventually, all that remains are small fragments of catalyst dispersed within a polyethylene matrix (Figure 2c).

Discussion

The topographical appearance of the silica support surface may be explained by taking into consideration its method of preparation via a sol−gel process.[1] The micelles formed during the syneresis stage of this preparative procedure vary in size from 3 to 50 nm, which undergo aggregation depending upon the exact conditions applied during the preparation.[18] The physical similarity between the silica support material and the calcined catalyst is indicative of its high thermal stability.

Although the Phillips CrO_x/silica catalyst is known to possess a wide range of chromium sites, only a small percentage are believed to be active.[5] This helps to explain why polyethylene

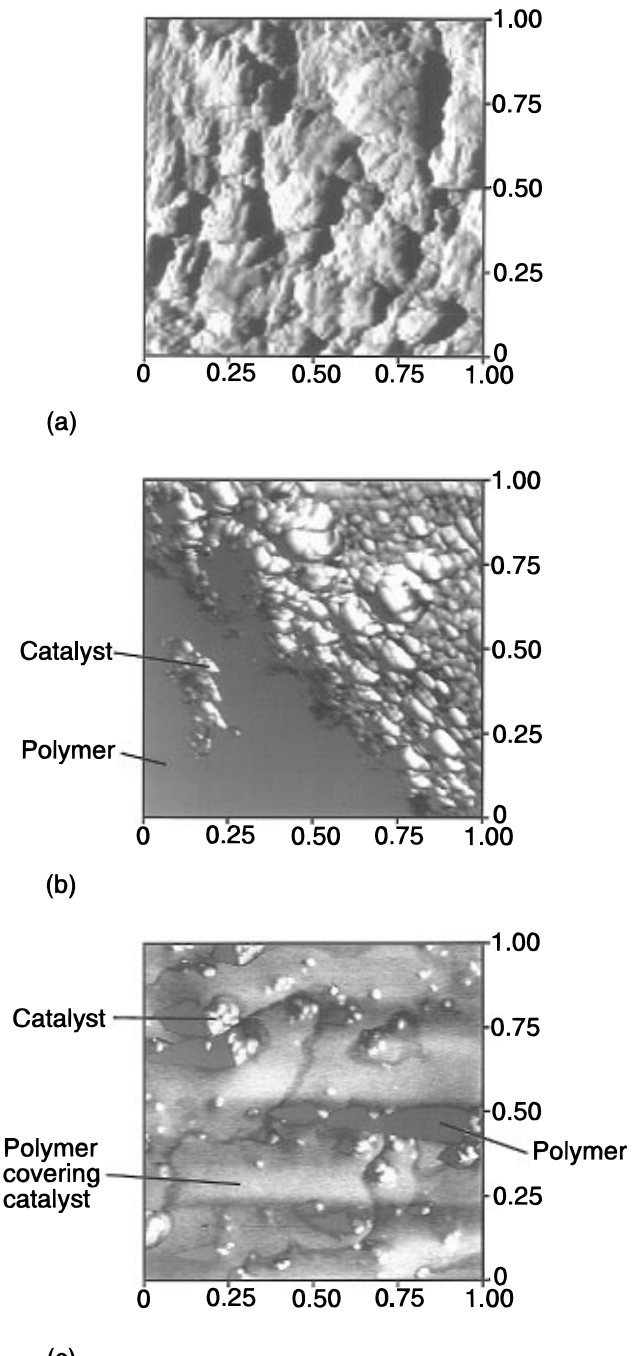

Figure 2. Phase-imaging AFM of the calcined CrO_x/silica catalyst at increasing stages of ethylene polymerization (where (a) corresponds to the catalyst surface prior to exposure of ethylene and the degree of shading is representative of different phases).

polymerization is not homogeneous across the catalyst surface. Also, the polymerization reaction is a highly exothermic process, while the catalyst particles are thermally insulating. This can lead to localized melting of the polymer,[8,11] which can give rise to agglomeration of polymerizing particles (as seen by optical microscopy).[9,11] Such agglomeration is very difficult to avoid but can be limited via efficient cooling and fragmentation of the catalyst during polymerization.[8,11] Diluting the monomer phase with an inert gas (argon was used in the present case) can lead to an improvement in cooling efficiency.

During the early stages of ethylene polymerization, the spheroidal catalyst features seen by AFM appear to fragment (Figure 2). Previous solid−gas chromatography[11] and mercury porosimetry[10] studies have shown that polymerization at low

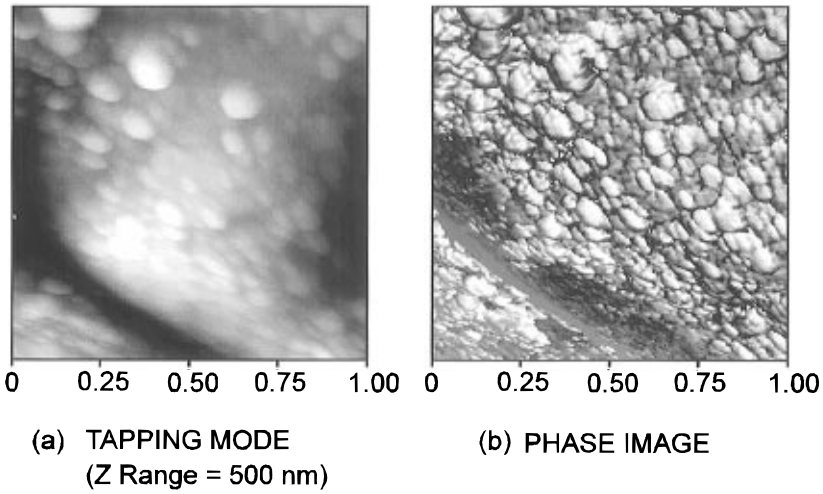

Figure 3. Polymer seeping through cracks extending from pores: (a) tapping mode AFM; (b) phase-imaging AFM.

yields fills the macropores of the catalyst nearest the external particle surface with polymer until there is a sufficient buildup of internal pressure for fragmentation to occur, resulting in fresh catalyst surface being exposed. This serves to increase monomer transport to active sites within the pores. Fragmentation produces trough-like features at the surface from which the polymer may then continue to grow[19] (Figure 3).

Previous studies using X-ray microscopy[8,9] and synchrotron microtomography[9] have suggested that large fragments of catalyst are concentrated toward the external surfaces of the growing polymer particles. Three different physical models for catalyst fragmentation have been put forward: (a) a "hard-core" model in which polymerization occurs around a nonfriable central catalyst particle; (b) a "uniform" site model in which small fragments are evenly distributed within the particle; (c) an "expanding-core" model in which convection of fragments to the exterior surface is caused by internal expansion.[20,21] The "hard-core" model is not applicable to the present study, since there is evidence for catalyst fragmentation. The "uniform" model requires homogeneous breakup of the catalyst particles to reach completion during the early stages of polymerization, combined with polymer growth at roughly equal rates around each fragment (this type of mechanism is reported for Ziegler−Natta type systems, where the catalyst friability is known to be high[22,23]). This may also be discounted in the present study, since nonuniform fragmentation of the catalyst is observed with small and large areas of the catalyst evident among the growing polymer (Figure 2b). The expanding core model is therefore most applicable to the CrO_x/silica polymerization catalyst. Such nonuniform fragmentation can lead to catalyst fragments possessing differing activities; the larger regions being less active than the smaller ones.[9,19] This can be attributed to the rate of polymerization being greater around the outer shell of catalyst fragments compared to the less monomer-accessible core region. Therefore, one would expect the rate of polymerization to increase with rising levels of catalyst fragmentation, since smaller particles have a higher surface area.[5] Concurrently, the less active large fragments will be convected toward the surface of the growing polymer particle via differential expansion;[8,9] upon reaching the surface, these large fragments become more accessible to monomer, providing a further buildup of polymer followed by fragmentation until eventually all that remains are very small catalyst moieties at the growing polymer particle surface (Figure 2c). The intermediate-shaded region in the phase image at this stage can be assigned to much larger catalyst fragments that have become covered by a thin layer of growing polyethylene, while the darker phase corresponds to polyethylene expanding onto the surface from trough-like features (where the larger support fragments have cracked open along a pore).

Conclusions

Phase-imaging atomic force microsopy has been used to follow the different stages of ethylene polymerization over the Phillips CrO_x/silica catalyst. The catalyst undergoes continuous fragmentation during the formation of polymer with the larger fragments being pushed out toward the surface where they undergo further fragmentation.

References and Notes

(1) Marsden, C. E. *Preparation of Catalysts V*; Poncelot, G., Jacobs, P. A., Grange, P., Delman, B., Eds.; Elsevier: Amsterdam, 1991.
(2) Dalla Lana, I. G.; Szymura, J. A.; Zielinski, P. A. *Proc. Int. Congr. Catal., 10th* **1992**, 2329.
(3) Conner, W. C.; Laurence, R. L.; Naik, B.; Webb, S. W.; Weist, E. L. *Proc. Int. Congr. Catal., 9th* **1988**, 1866.
(4) McDaniel, M. P. *J. Polym. Sci., Polymer Chem. Ed.* **1981**, *19*, 1967.
(5) McDaniel, M. P. *Adv. Catal.* **1981**, *33*, 47.
(6) Niegisch, W. D.; Crisafulli, S. T.; Nagel, T. S.; Wagner, W. D. *Macromolecules* **1992**, *25*, 3910.
(7) Szymura, J. A.; Zielinski, P. A.; Dalla Lana, I. G. *Catal. Lett.* **1992**, *15*, 145.
(8) Webb, S. W.; Weist, E. L.; Chiovetta, M. G.; Laurence, R. L.; Conner, W. C. *Can. J. Chem. Eng.* **1991**, *69*, 665.
(9) Conner, W. C.; Webb, S. W.; Spanne, P.; Jones, K. W. *Macromolecules* **1990**, *23*, 4742.
(10) Weist, E. L.; Ali, A. H.; Conner, W. C. *Macromolecules* **1987**, *20*, 689.
(11) Webb, S. W.; Conner, W. C.; Laurence, R. L. *Macromolecules* **1989**, *22*, 2885.
(12) Binnig, G.; Quate, C. F.; Gerber, C. *Phys. Rev. Lett.* **1986**, *56* (9), 930.
(13) Chernoff, D. A. *Proc. Microsc. Microanal.* **1995**, 888.
(14) Chernoff, D. A. *Nanovations Winter 1996*; Digital Instruments: Santa Barbara, CA, 1996; p 6.
(15) Thundat, T.; Zheng, X. Y.; Sharp, S. L.; Allison, D. P.; Warnack, R. J.; Joy, P. I.; Ferrell, T. L. *Scanning Microsc.* **1992**, *6*, 903.
(16) Shakesheff, K. M.; Davies, M. C.; Jackson, D. E.; Roberts, C. J.; Tendler, S. J. B.; Brown, V. A.; Watson, R. C.; Barrett, D. A.; Shaw, P. N. *Surf. Sci. Lett.* **1994**, *304*, L393.
(17) Koenig, J. L. *Chemical Microstructure of Polymer Chains*; Wiley: New York, 1980; p 199.
(18) Winyall, M. E. *Applied Industrial Catalysis*; Academic: New York, 1984; Vol. 3, Chapter 3.
(19) Follestad, A.; Helleborg, S.; Almquist, V. *Stud. Surf. Sci. Catal.* **1990**, *56*, 63.
(20) Singh, D.; Merrill, R. P. *Macromolecules* **1971**, *4*, 599.
(21) Schmeal, W. R.; Street, J. R. *AIChE J.* **1971**, *17* (5), 1188.
(22) Kakugo, M.; Sadatoshi, H.; Yokoyama, M.; Kojima, K. *Macromolecules* **1989**, *22*, 547.
(23) Kakugo, M.; Sadatoshi, H.; Sakai, J.; Yokoyama, M. *Macromolecules* **1989**, *22*, 3172.